

Effect of anisotropic Fermi surface on the flux-flow resistivity under rotating magnetic field

Y. Higashi^{a,c,*} Y. Nagai^b M. Machida^b N. Hayashi^c

^a Department of Mathematical Sciences, Osaka Prefecture University, 1-1 Gakuen-cho, Naka-ku, Sakai 599-8531, Japan

^b CCSE, Japan Atomic Energy Agency, 5-1-5 Kashiwanoha, Kashiwa, Chiba 277-8587, Japan

^c NanoSquare Research Center (N2RC), Osaka Prefecture University, 1-2 Gakuen-cho, Naka-ku, Sakai 599-8570, Japan

Abstract

We numerically investigate the effect of in-plane anisotropic Fermi surface (FS) on the flux-flow resistivity ρ_f under rotating magnetic field on the basis of the quasiclassical Green's function method. We demonstrate that one can detect the phase in pairing potential of Cooper pair through the field-angular dependence of ρ_f even if the FS has in-plane anisotropy. In addition, we point out one can detect the gap-node directions irrespective of the FS anisotropy by measuring ρ_f under rotating field.

Key words: Field-angle dependent measurement; Flux-flow resistivity; Phase-sensitive probe

PACS: 74.20.Rp, 74.25.Op, 74.25.nn

1. Introduction

It is important task to clarify the internal degree of freedom for the orbital part of Cooper pair wave function, which is the fundamental nature of superconductivity. We have ever proposed a new experimental method to detect both the phase and the anisotropy of pairing potential. That is, we have investigated the in-plane magnetic field-angle dependence of the quasiparticle scattering rate inside a vortex core [1] and the flux-flow resistivity ρ_f [2]. Through a series of our researches, we obtained the knowledge that the field-angle dependence of ρ_f is sensitive to the phase of pairing potential both in the cases of an isotropic and an uniaxially anisotropic Fermi surface (FS). The field-angle de-

pendence of ρ_f has not been investigated yet for an in-plane anisotropic FS.

In this paper, we investigate effects of in-plane FS anisotropy on the field-angle dependence of flux-flow resistivity $\rho_f(\alpha_M)$. Most materials have the anisotropy in their FS reflecting the anisotropy of crystal structures. Thus, it is more realistic to investigate $\rho_f(\alpha_M)$ in the case of anisotropic FS. We consider two model FSs with in-plane anisotropy and numerically calculate $\rho_f(\alpha_M)$ for those FSs with changing the anisotropy of FS. Our numerical results show that one can detect the gap-node direction by measuring ρ_f under rotating magnetic field even if the FS has an anisotropy.

2. Formulation

We consider a single vortex at low magnetic field and at low temperature. The energy dissipation due to the vortex flow comes from non-magnetic impurity scattering within a vortex core. Two contribu-

* Corresponding author. N2RC, Osaka Prefecture University, C10 Bldg., 1-2 Gakuen-cho, Naka-ku, Sakai 599-8570, Japan Tel.: +81-72-254-9829 ; fax: +81-72-254-8203.

Email address: higashiyoichi@ms.osakafu-u.ac.jp (Y. Higashi).

tions to the flux-flow resistivity ρ_f are considered [2]. One is the quasiparticle scattering due to randomly distributed impurities [1,3] and the other is the energy scale of the quasiparticle (QP) bound states inside a vortex core $\omega_0(\mathbf{k}_F)$ [2,4]. Note that this energy scale depends on the wave vector [5] within the framework of the quasiclassical theory of superconductivity.

We assume an isotropic vortex characterized by the pair potential given as $\Delta(\mathbf{r}, \mathbf{k}_F) = |\Delta(\mathbf{r})|d(\mathbf{k}_F)e^{i\phi(|\mathbf{r}|)}$. We set $|\Delta(\mathbf{r})| = \Delta_\infty \tanh(|\mathbf{r}|/\xi)$ as the spatial variation of the pair potential amplitude. Δ_∞ is the bulk amplitude, ξ is the coherence length, and $\phi(|\mathbf{r}|)$ is the azimuthal angle in the real space. $d(\mathbf{k}_F)$ denotes the anisotropy of the pair potential in the \mathbf{k} -space. \mathbf{k}_F is the Fermi wave vector.

The expression for the flux-flow resistivity ρ_f is given as [2]

$$\rho_f(T) \propto \frac{1}{\left\langle \frac{\omega_0(\mathbf{k}_F)}{\Gamma(\varepsilon = k_B T, \mathbf{k}_F)} \right\rangle_{\text{FS}}}, \quad (1)$$

where the integral on a FS with respect to \mathbf{k}_F is $\langle \dots \rangle = (1/\nu_0) \int dS_F / |\mathbf{v}_F(\mathbf{k}_F)| \dots$. The area element on an anisotropic FS is $dS_F = |\mathbf{k}_F(\phi_k, \theta_k)|^2 \sin \theta_k d\phi_k d\theta_k$. The total density of state on a FS is $\nu_0 = \int dS_F / |\mathbf{v}_F(\mathbf{k}_F)|$. The Fermi velocity is $\mathbf{v}_F(\mathbf{k}_F) = \nabla_{\mathbf{k}} \epsilon(\mathbf{k})|_{\mathbf{k}=\mathbf{k}_F}$. In this paper, we use a unit system in which $\hbar = 1$. Here, we assume that the system is in moderately clean regime and that quasiparticles with energy $\varepsilon = k_B T$ predominantly contribute to the flux-flow resistivity at the temperature T [6]. Within the quasiclassical theory, the momentum dependent interlevel spacing of the vortex bound states $\omega_0(\mathbf{k}_F)$ is obtained by using Kramer-Pesch approximation [7] as $\omega_0(\mathbf{k}_F) = 2|d(\mathbf{k}_F)|^2 \Delta_\infty^2 / (|\mathbf{k}_{F\perp}| |\mathbf{v}_{F\perp}(\mathbf{k}_F)|)$ [2,3]. Here, $\mathbf{k}_{F\perp}$ and $\mathbf{v}_{F\perp}$ are the components of \mathbf{k}_F and \mathbf{v}_F projected onto the plane perpendicular to \mathbf{H} , respectively. The quasiparticle scattering rate inside a vortex core Γ is given by [1,3]

$$\Gamma(\varepsilon) = \frac{\pi}{2} \Gamma_n \left\langle \left\langle (1 - \text{sgn}[d(\mathbf{k}_F)d(\mathbf{k}'_F)] \cos \Theta) \times \frac{1}{|\sin \Theta|} \frac{|\mathbf{v}_{F\perp}(\mathbf{k}'_F)| |d(\mathbf{k}_F)|}{|\mathbf{v}_{F\perp}(\mathbf{k}_F)| |d(\mathbf{k}'_F)|} \times e^{-u(s_0, \mathbf{k}_F)} e^{-u(s'_0, \mathbf{k}'_F)} \right\rangle_{\text{FS}'} \right\rangle_{\text{FS}}, \quad (2)$$

where Γ_n is the scattering rate in the normal state, $\Theta(\mathbf{k}_F, \mathbf{k}'_F) \equiv \theta_v(\mathbf{k}_F) - \theta_v(\mathbf{k}'_F)$ is the scattering angle

and $u(s, \mathbf{k}_F) = (2|d(\mathbf{k}_F)|/|\mathbf{v}_{F\perp}(\mathbf{k}_F)|) \int_0^{|s|} ds' \Delta(s')$ with $\Delta(s') = \Delta_\infty \tanh(s'/\xi)$. s' is the real space coordinate along the QP trajectory. One can obtain further information on the expression of Γ in Ref. [1,3].

We consider two model FSs I, II with in-plane anisotropy. The model FS I is characterized by the energy dispersion $\epsilon_I(\mathbf{k}) = -\mu_I - 2t \{\cos(k_x a) + \cos(k_y a)\} + k_z^2/(2m)$, where t and a are the hopping integral and the lattice constant, respectively. μ_I is the chemical potential. The dispersion in the $k_x - k_y$ plane is given by the tight-binding (TB) model and that in the k_z direction is free electron model. As characteristics of the TB model, there are Van Hove singularities in the direction of $(\pi, 0)$ and $(0, \pi)$, at which $|\nabla_{\mathbf{k}} \epsilon(\mathbf{k})| = 0$ [8]. In addition to this point, the anisotropy of the FS grows larger gradually with increasing the chemical potential below the half filling. The model FS II is given by the anisotropic dispersion $\epsilon_{II}(\mathbf{k}) = -\mu_{II} + 1/(2m) \{k_x^2 + k_y^2 + a^2(k_x^4 + k_y^4)/2 + 3a^2 k_x^2 k_y^2 + k_z^2\}$ [9,10]. m is the mass of charge. In numerical calculation, we set the parameter $mta^2 = 1$.

For an isotropic FS, the position on the FS is identified by the azimuthal and the polar angle (ϕ_k, θ_k) . However, in anisotropic FSs, it is identified by ϕ_k, θ_k and the Fermi radius $|\mathbf{k}_F(\phi_k, \theta_k)|$. We can parametrize the Fermi wave numbers in spherical coordinates: $k_{Fx} = |\mathbf{k}_F(\phi_k, \theta_k)| \cos \phi_k \sin \theta_k$, $k_{Fy} = |\mathbf{k}_F(\phi_k, \theta_k)| \sin \phi_k \sin \theta_k$, $k_{Fz} = |\mathbf{k}_F(\phi_k, \theta_k)| \cos \theta_k$. Substituting these Fermi wave numbers into the above two dispersions $\epsilon_I(\mathbf{k})$ and $\epsilon_{II}(\mathbf{k})$, and using a bisection method, we can determine numerically $|\mathbf{k}_F(\phi_k, \theta_k)|$ such that $\epsilon(\mathbf{k}) = 0$.

For FS I, the absolute value of the Fermi velocity is

$$|\mathbf{v}_F(\phi_k, \theta_k)| = 2ta \sqrt{\sin^2(k_{Fx}a) + \sin^2(k_{Fy}a) + \frac{1}{4(mta^2)^2} k_{Fz}^2} \quad (3)$$

and for FS II,

$$|\mathbf{v}_F(\phi_k, \theta_k)| = \frac{1}{m} \left\{ k_{Fx}^2 (1 + a^2 k_{Fx}^2 + 3a^2 k_{Fy}^2)^2 + k_{Fy}^2 (1 + a^2 k_{Fy}^2 + 3a^2 k_{Fx}^2)^2 + k_{Fz}^2 \right\}^{1/2} \quad (4)$$

When integrating Eq. (2) numerically, we need a relation between $\mathbf{v}_{F\perp}(\phi_k, \theta_k)$ and $\mathbf{v}_F(\phi_k, \theta_k)$ [1]. The component of $\mathbf{v}_F(\phi_k, \theta_k)$ projected onto the plane perpendicular to \mathbf{H} is given by

$$\begin{aligned}
|\mathbf{v}_{F\perp}(\phi_k, \theta_k)| &= |\mathbf{v}_F(\phi_k, \theta_k)| \\
&\quad \times \sqrt{\cos^2 \theta_k + \sin^2 \theta_k \sin^2(\phi_k - \alpha_M)} \quad (5) \\
\cos \theta_v(\mathbf{k}_F) &= -\frac{|\mathbf{v}_F(\phi_k, \theta_k)|}{|\mathbf{v}_{F\perp}(\phi_k, \theta_k)|} \cos \theta_k, \quad (6) \\
\sin \theta_v(\mathbf{k}_F) &= \frac{|\mathbf{v}_F(\phi_k, \theta_k)|}{|\mathbf{v}_{F\perp}(\phi_k, \theta_k)|} \sin \theta_k \sin(\phi_k - \alpha_M) \quad (7)
\end{aligned}$$

where $\theta_v(\mathbf{k}_F)$ is the angle of the QP trajectory measured from the \mathbf{a}_M -axis. The \mathbf{a}_M - \mathbf{b}_M plane is perpendicular to \mathbf{H} ($\mathbf{c}_M \parallel \mathbf{H}$). α_M is the magnetic field angle measured from the $(\pi, 0)$ direction.

In order to investigate the relation between the anisotropy of the pair potential and that of the FSs, we consider the following four model pair potentials: (i) Line-node $s_{|x^2-y^2|}$ -wave: $d(\mathbf{k}_F) = |\cos(2\phi_k) \sin^2 \theta_k|$, (ii) Line-node $s_{|xy|}$ -wave: $d(\mathbf{k}_F) = |\sin(2\phi_k) \sin^2 \theta_k|$, (iii) $d_{x^2-y^2}$ -wave: $d(\mathbf{k}_F) = \cos(2\phi_k) \sin^2 \theta_k$, and (iv) d_{xy} -wave: $d(\mathbf{k}_F) = \sin(2\phi_k) \sin^2 \theta_k$. While $s_{|x^2-y^2|}$ ($s_{|xy|}$)-wave and $d_{x^2-y^2}$ (d_{xy})-wave pair potentials have the same anisotropy, only $d_{x^2-y^2}$ (d_{xy})-wave one has the sign change. $s_{|x^2-y^2|}$ ($d_{x^2-y^2}$)-wave pair potential coincides with $s_{|xy|}$ (d_{xy})-wave one when the pair potential is rotated by $\pi/4$ [rad].

3. Results

In Figs. 1 and 2, we show the numerical results of the field-angle α_M dependence of the flux-flow resistivity ρ_f for the model FS I and II. The inset shows the schematic figure of the pair potential on the anisotropic FS. We fix the temperature in this calculation at $T = 0.35T_C$. Each plot corresponds to different chemical potential. For the energy dispersion II, the chemical potential μ_{II} is fixed to $\mu_{II} = 9t$.

In Figs. 1(a) and 1(b), we can see that ρ_f has the maximum value when \mathbf{H} is applied parallel to the gap-node direction. This behavior in the $s_{|x^2-y^2|}$ -wave pair is consistent with the result for both an isotropic and an uniaxially anisotropic FS [2]. The same behavior is seen also for the $d_{x^2-y^2}$ and the d_{xy} -wave pair [see Fig. 2(a) and 2(b)]. However, the oscillation amplitude of $\rho_f(\alpha_M)$ for the $d_{x^2-y^2}$ and the d_{xy} -wave pair becomes larger than that for the $s_{|x^2-y^2|}$ and the $s_{|xy|}$ -wave one. In addition, for the $d_{x^2-y^2}$ -wave pair, a rather sharper peak appears when $\mathbf{H} \parallel \pi/4$. These characteristics originate from the sign-change in the pair potential because its amplitude is the same between the $s_{|x^2-y^2|}$ and the $d_{x^2-y^2}$ (or the $s_{|xy|}$ and the d_{xy})-wave pair.

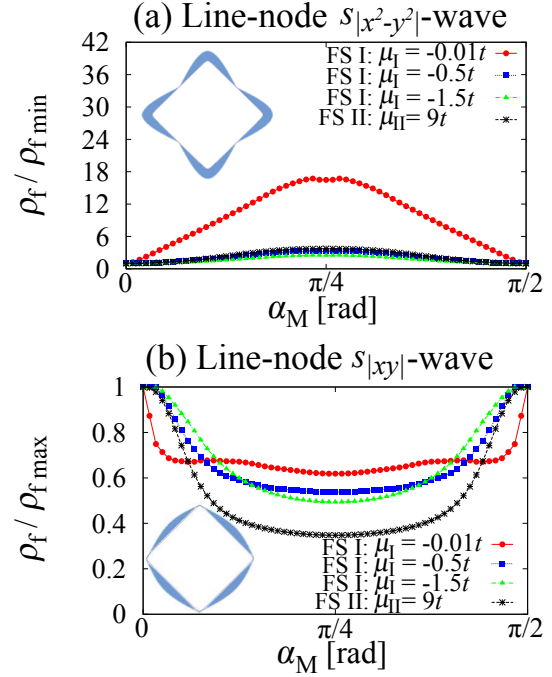


Fig. 1. The field angle α_M dependence of the flux-flow resistivity ρ_f in the case of the (a) line-node $s_{|x^2-y^2|}$ -wave pair and the (b) line-node $s_{|xy|}$ -wave one. The temperature is set to $T = 0.35T_C$. Each curve is plotted for the different chemical potential. For FS II, the chemical potential is set to $\mu_{II} = 9t$. The vertical axis is normalized by (a) minimum value and (b) maximum value for each curve.

We notice that the curve of $\rho_f(\alpha_M)$ for FS I approaches the curve for FS II with decreasing the FS anisotropy ($\mu_I = -0.01t \rightarrow -1.5t$) in Figs. 1 and 2. The anisotropy of FS II with $\mu_{II} = 9t$ is almost the same as that of FS I with $\mu_I = -1.5t$. The cusplike sharp peak appearing in an isotropic FS for the $d_{x^2-y^2}$ -wave pair [2] is not observed in the case of these in-plane anisotropic FSs. For any pairing states, when $\mathbf{H} \parallel$ gap node, the peak becomes sharp with increasing the anisotropy of the FS. We consider that this behavior comes from the anisotropy of the FS. The important point is that one can detect the gap-node direction from the field-angle dependence of the flux-flow resistivity even if there is an anisotropy of a FS. That is, a peak of $\rho_f(\alpha_M)$ appears in the gap-node direction irrespective of a FS anisotropy.

4. Summary

We investigated the field-angle dependence of the flux-flow resistivity for two models of FSs. As a result, we find that the maximum value of $\rho_f(\alpha_M)$ al-

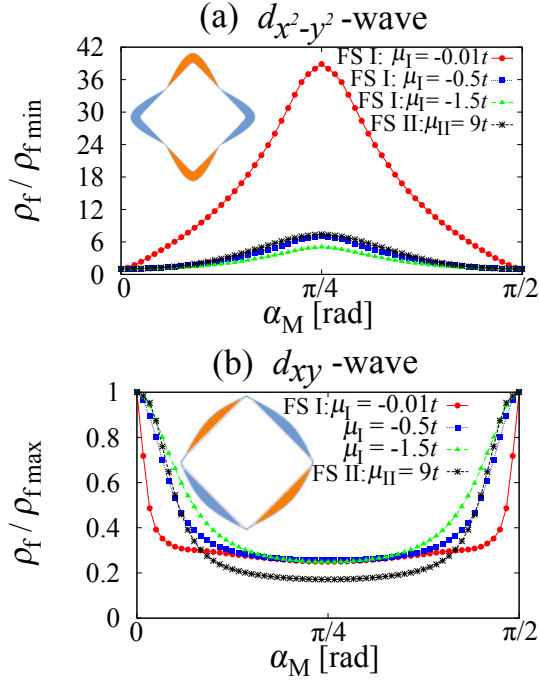


Fig. 2. The field angle α_M dependence of the flux-flow resistivity ρ_f in the case of the (a) $d_{|x^2-y^2|}$ -wave pair and the (b) $d_{|xy|}$ -wave one. The temperature is set to $T = 0.35T_c$. Each curve is plotted for the different chemical potential. For FS II, the chemical potential is set to $\mu_{II} = 9t$. The vertical axis is normalized by (a) minimum value and (b) maximum value for each curve.

ways appears when \mathbf{H} is oriented parallel to the gap-node direction even if the FS has an anisotropy. This result is irrespective of the relation between the anisotropy of the pair potential and that of the FS [compare Fig. 1(a) with 1(b) and Fig. 2(a) with 2(b)].

Acknowledgments

The authors thank N. Nakai, H. Suematsu, T. Okada, S. Yasuzuka, Y. Kato, K. Izawa, M. Kato, and A. Maeda for helpful discussions.

References

- [1] Y. Higashi, Y. Nagai, M. Machida, N. Hayashi, *Physica C* 471 (2011) 828; *Physica C*, in press [<http://dx.doi.org/10.1016/j.physc.2012.02.006>].
- [2] Y. Higashi, Y. Nagai, M. Machida, N. Hayashi, in preparation; *J. Phys.: Conf. Ser.* 400 (2012) 022025.
- [3] Y. Nagai, Y. Kato, *Phys. Rev. B* 82 (2010) 174507.
- [4] N. B. Kopnin, G. E. Volovik, *Phys. Rev. Lett.* 79 (1997) 1377; Yu. G. Makhlin, *Phys. Rev. B* 56 (1997) 11872;

- N. B. Kopnin, G. E. Volovik, *Ü. Parts, Europhys. Lett.* 32 (1995) 651; Alan T. Dorsey, *Phys. Rev. B* 46 (1992) 8376.
- [5] G. E. Volovik, *Pis'ma Zh. Eksp. Teor. Fiz.* 70 (1999) 601 [*JETP Lett.* 70 (1999) 609]; N. B. Kopnin, G. E. Volovik, *Pis'ma Zh. Eksp. Teor. Fiz.* 64 (1996) 641 [*JETP Lett.* 64 (1996) 690].
- [6] Y. Kato, *J. Phys. Soc. Jpn.* 69 (2000) 3378.
- [7] Y. Nagai, N. Hayashi, *Phys. Rev. Lett.* 101 (2008) 097001; Y. Nagai, Y. Ueno, Y. Kato, N. Hayashi, *J. Phys. Soc. Jpn.* 75 (2006) 104701, and references therein.
- [8] J. Sadowski, Master Thesis (University of Saskatchewan, 2011); N. W. Ashcroft, N. D. Mermin, *Solid State Physics* (Thomson Learning, 1976).
- [9] I. Vekhter, A. Vorontsov, *Physica B* 403 (2008) 958.
- [10] We rotate the model FS given in Ref. [9] by $\pi/4$ [rad] within the $k_x - k_y$ plane in order to compare the result for FS II with that for FS I.